Collisional damping rates for electron plasma waves reassessed

J. W. Banks, S. Brunner, R. L. Berger, W. J. Arrighi, and T. M. Tran

Phys. Rev. E **96**, 043208 — Published 13 October 2017

DOI: 10.1103/PhysRevE.96.043208

Collisional Damping Rates for Electron Plasma Waves Reassessed

J. W. Banks[1],* S. Brunner[2], R. L. Berger[3], W. J. Arrighi[3], and T. M. Tran[2]
(1) Rensselaer Polytechnic Institute,
Department of Mathematical Sciences, Troy, NY 12180
(2) Ecole Polytechnique Fédérale de Lausanne (EPFL),
Swiss Plasma Center (SPC),
CH-1015 Lausanne, Switzerland and
(3) Lawrence Livermore National Laboratory, P.O. Box 808, Livermore, California 94551
(Dated: September 28, 2017)

Collisional damping of electron plasma waves, the primary damping for high phase velocity waves, is proportional to the electron-ion collision rate, $\nu_{ei,th}$. Here, it is shown that the damping rate normalized to $\nu_{ei,th}$ depends on the charge state, Z, on the magnitude of $\nu_{ei,th}$ and the wavenumber k in contrast with the commonly used damping rate in plasma wave research. Only for weak collision rates in low-Z plasmas for which the electron self-collision rate is comparable to the electron-ion collision rate is the damping rate given by the commonly accepted value. The result presented here corrects the result presented in textbooks at least as early as 1973. The complete linear theory requires the inclusion of both electron-ion pitch-angle and electron-electron scattering, which itself contains contributions to both pitch angle scattering and thermalization.

I. INTRODUCTION

Collisions may provide the only significant damping of electron plasma waves (EPWs) in low-temperature laboratory plasmas, for EPWs driven by stimulated Raman scatter (SRS), either forward scatter or backscatter near the quarter-critical surface, and for the higher phase velocity EPW in the two-plasmon decay (TPD) instability, that is, whenever the phase velocity of the EPW is greater than 4-5 times the electron thermal velocity. Forward Raman scatter is also a concern to the efficient performance of the Backward Raman Amplifier.[1, 2] SRS and TPD are of particular concern for direct-drive Inertial Confinement Fusion because of both the loss of drive resulting from the energy lost to SRS, and the preheat of the fuel by energetic electrons.[3–5] Recent National Ignition Facility designs have added a high-Z material layer to the capsule ablator to increase the collisional damping of EPWs in an attempt to suppress TPD.[6] The implications of our results for collisional damping on the TPD threshold and on nonlinear TPD saturation mechanisms will be discussed in the conclusions.

The effect of weak collisions on the linear Landau damping of EPWs has been the subject of a number of publications since the 1960s.[7–13] Comparatively little attention has been given to collisional damping perhaps because of the assumed result that the damping rate is one-half the velocity-weighted collision rate averaged over a Maxwell-Boltzmann distribution of electrons.[14] That is $\nu^{fl}_{\rm coll} \simeq \nu^{\rm brag}_{ei}/2$ where $\nu^{\rm brag}_{ei}$ is the electron-ion scattering rate as defined by Braginskii.[15]

Previously, using the 2D+2V Vlasov code LOKI, we found that for plasmas without self-collisions, the collisional damping of EPWs was less than the commonly assumed ν^{fl}_{coll}.[16] However, that result had limited applicability for two reasons. First, only the electron-ion scattering operator restricted to two Cartesian velocity dimensions (v_x, v_y) was considered. As will be shown here, there are significant differences in the damping rate in high-Z limit between the Cartesian collision operator restricted to 2V and the full 3V operator used in this work. Second, the important electron-electron scattering operator, essential to the standard "textbook" theory, was neglected. Here, to our knowledge for the first time in a Vlasov code, we include both electron-ion and electron-electron operators.

In agreement with previous work we find that weak collisions do not reduce Landau damping. Here, within the context of the Landau Collision operator, we extend the applicability of that result to collision rates as large as one-half the plasma frequency. Concerning the collisional damping rate, we find that $\nu_{\rm coll}/\nu^{fl}_{\rm coll}$ is a function of ionization state Z, varying from ~ 1 at $Z = 1$ to ~ 0.7 as $Z \to \infty$ for strongly collisional plasmas. This $Z-$dependence should be expected because electron-ion collisions only isotropize the distribution whereas electron-electron collisions drive the distribution towards a Maxwell-Boltzmann.

For weak collisions, the exponential decay rate of the perturbation is in accord with the linear Landau damping rate ν_L for an EPW. For larger collision rates, we find an increase in the damping rate above ν_L, as expected from the additional effects of collisional damping. However, we find that even with the full collision operator employing both electron-ion (pitch-angle) and electron-electron (pitch-angle and thermalization) collision operators, the damping directly attributable to collisions for $Z \gtrsim 6$ is 70-90% of $\nu^{fl}_{\rm coll}$, the rate derived from a linearized set of fluid equations with electron-ion momentum exchange, Eqs (38)-(43) in Ref. [16]. The greater reduction occurs with larger collision rates. Only if $Z \lesssim 4$ is the collisional damping well-approximated by $\nu^{fl}_{\rm coll}$. The transition of

*banksj3@rpi.edu

$\nu_{\rm coll}$ to the asymptotic rate as a function of Z is well approximated by an exponential decrease such that the $Z \to \infty$ rate is approached within 20% for Z as small as 6 (for a fixed value of $\nu_{ei,th}$). The remainder of this paper is organized as follows. Sec. II presents a concise description of the mathematical formulation of the governing equations discretized in the Vlasov simulation code. Sec. III then shows results of Vlasov simulations of the damping of EPWs for varying charge states Z, collision rates, and wavenumbers. Finally in Sec. IV, we provide a summary of the results and discussion of applications.

II. VLASOV SIMULATION AND METHOD

In this work, we use a 1D+3V Vlasov code in cylindrical velocity coordinates and assume azimuthal symmetry to effectively reduce the system to one spatial (x) and two velocity coordinates ($v_x, v_\perp$). A few results from the 2D+2V LOKI code extended to include self-collisions will also be presented to facilitate discussion of multi-dimensional simulations in the conclusions. Including both electron-ion and electron-electron collision operators, we compute the damping rate of an initial small-amplitude EPW (initialized with a small-amplitude density perturbation). The effects of collisions on EPW damping are discussed for a range of Z and thermal electron-ion collision frequency, $\nu_{ei,th}/\omega_{pe}$, where $\omega_{pe} = \sqrt{4\pi N_e e^2/m_e}$ is the electron plasma frequency and

$$\nu_{ei,th} \;=\; 2\pi \frac{Ze^4 N_e \ln(\Lambda_{ei})}{m_e^2 v_{\rm th\,e}^3}. \tag{1}$$

Here $-e$ is the elementary electric charge of the electron, m_e its mass, and $v_{\rm th\,e} = \sqrt{T_e/m_e}$ the electron thermal velocity. Further, T_e is the electron temperature and N_e is the spatially-averaged background electron density. The thermal electron self-collision rate is $\nu_{ee,th} = 8\pi e^4 N_e \ln(\Lambda_{ee})/(m_e^2 v_{\rm th\,e}^3)$, and $\ln(\Lambda_{ei})$ and $\ln(\Lambda_{ee})$ are the Coulomb logarithms for electron-ion and electron-electron collisions respectively. Note that we have adopted CGS units throughout, and that $\nu_{ei}^{\rm brag} = [4/(3\sqrt{2\pi}]\nu_{ei,th} \simeq 0.532\nu_{ei,th}$.

The evolution of the electron distribution function $f(x, v_x, v_\perp, t)$ is described by the Fokker-Planck equation, *i.e.* the Vlasov equation including collisional effects:

$$\frac{\partial f}{\partial t} + \vec{v}\cdot\nabla f - \frac{e}{m_e}\vec{E}\cdot\frac{\partial}{\partial \vec{v}} f = -C_{ee}[f,f] - C_{ei} f. \tag{2}$$

The electric field components, $\vec{E} = -\nabla\phi$ are obtained from the electrostatic potential, $\phi(x,t)$, which is itself determined by Poisson's equation, $\nabla^2\phi = 4\pi e\left(\int f_e\, d\vec{v} - N_i Z\right)$, where we have assumed a single immobile ion species with homogeneous density N_i and charge Ze, ensuring charge neutrality over the physical domain.

In Eq. (2), electron-ion pitch angle scattering is described by the Lorentz operator,

$$C_{ei}\,(f) \;=\; -\nu_{ei,th}\, v_{\rm th\,e}^3 \frac{\partial}{\partial \vec{v}}\cdot \mathbf{U}\cdot\frac{\partial f}{\partial \vec{v}}. \tag{3}$$

The tensor $\mathbf{U}$ is defined as

$$\mathbf{U}(\vec{v}) = \frac{1}{v}\left(\mathbf{I} - \frac{\vec{v}:\vec{v}}{v^2}\right), \tag{4}$$

where $\vec{v}$ is the velocity vector, v its amplitude and $\mathbf{I}$ the identity tensor.

In this work the nonlinear self-collision Landau operator $C_{ee}[f,f]$, bilinear in its two arguments, is linearized with respect to the spatially uniform Maxwellian distribution $f_{\rm M}(v) = N_e \exp[-v^2/(2v_{\rm th\,e}^2)]/[(2\pi)^{3/2} v_{\rm th\,e}^3]$. Note that $C_{ee}[f_{\rm M}, f_{\rm M}] = 0$ for any Maxwellian distribution. The linearized operator, denoted $\hat{C}_{ee}(f)$, is given by

$$\hat{C}_{ee}(f) = C_{ee}[f_{\rm M}, f] + C_{ee}[f, f_{\rm M}],$$

where $C_{ee}[f_M, f]$ represents collisions of the deviation $\delta f = f - f_{\rm M}$ on the Maxwellian background $f_{\rm M}$, while the second term $C_{ee}[f, f_{\rm M}]$, the so-called back-reaction, represents the collisions of the Maxwellian background $f_{\rm M}$ on the fraction δf. The first term can be cast in self-adjoint differential form operating on f as

$$C_{ee}[f_{\rm M}, f] = -\frac{\partial}{\partial \vec{v}}\cdot\left[f_{\rm M}(v)\,\mathbf{D}_{ee}\cdot\frac{\partial}{\partial \vec{v}}\left(\frac{f(\vec{v})}{f_{\rm M}(v)}\right)\right]. \tag{5}$$

The diffusion tensor $\mathbf{D}_{ee}$ is derived analytically for the assumed Maxwellian background as

$$\begin{aligned}\mathbf{D}_{ee} &= \gamma_{ee}\int d\vec{v}\,' f_{\rm M}(\vec{v}\,')\mathbf{U}(\vec{v}-\vec{v}\,') \\ &= \frac{N_e\,\gamma_{ee}}{v_{\rm th\,e}}\left[K(\mathsf{v})\left(\mathbf{1} - \frac{\vec{v}:\vec{v}}{v^2}\right) + 2\,H(\mathsf{v})\,\frac{\vec{v}:\vec{v}}{v^2}\right],\end{aligned}$$

with $\gamma_{ee} = \nu_{ee,th} v_{\rm th\,e}^3/(4N_e)$ and the normalized velocity amplitude, $\mathsf{v} = v/v_{\rm th\,e}$. The functions $H(\mathsf{v})$ and $K(\mathsf{v})$ are related to the Rosenbluth potentials [17] and given in [18]. The contributions to $\mathbf{D}_{ee}$ proportional to $H(\mathsf{v})$ and $K(\mathsf{v})$ correspond respectively to thermalization and pitch angle scattering.

The back-reaction term, $C_{ee}[f, f_{\rm M}]$, is essential to ensure conservation of mass, momentum, and kinetic energy, but the exact (Landau) form is an integral equation that is numerically cumbersome. Therefore, as in Refs. [19, 20], we have used the following approximate simplified operator:

$$\begin{aligned}C_{ee}[f, f_{\rm M}] \simeq &-\frac{C_{ee}[f_{\rm M}, \vec{v} f_{\rm M}]\cdot\int d\vec{v}\,'\, C_{\rm ee}[f_{\rm M}, \vec{v}\,' f_{\rm M}]\,\frac{f(\vec{v}\,')}{f_{\rm M}(v')}}{\frac{1}{V}\int d\vec{v}\,'\, C_{\rm ee}[f_{\rm M}, \vec{v}\,' f_{\rm M}]\cdot\vec{v}\,'} \\ &- \frac{C_{ee}[f_{\rm M}, v^2 f_{\rm M}]\int d\vec{v}\,'\, C_{\rm ee}[f_{\rm M}, v'^2 f_{\rm M}]\,\frac{f(\vec{v}\,')}{f_{\rm M}(v')}}{\int d\vec{v}\,'\, C_{\rm ee}[f_{\rm M}, v'^2 f_{\rm M}] v'^2},\end{aligned} \tag{6}$$

where V is the dimensionality of velocity space (discussed in the conclusions). Note that in Eq. (6), the operator $C_{ee}[\cdot, f_{\rm M}]$ is fully expressed in terms of the operator $C_{ee}[f_{\rm M}, \cdot]$ given by Eq. (5). Invoking the symmetry of the operator $C_{ee}[f_{\rm M}, \cdot]$ one can prove that the linearized operator $\hat{C}_{ee}(f)$ with the approximate back-reaction term (6) possesses the same symmetry and conservation properties as the original integral operator. These properties ensure that linearized shifted Maxwellian distributions remain exact stationary states of the operator $\hat{C}_{ee}(f)$.[18] By then applying a consistent and accurate discretization approach, one ensures that these properties are preserved in the numerical approximation.

III. RESULTS

Consider now the effect of collisions on linear damping of spatially one-dimensional EPWs propagating in the x-direction with wavenumber $k\lambda_{De} = 0.3$. We present simulation results obtained with an initial electron distribution set to

$$f(x, v_x, v_\perp, t = 0) = \left[1 + \frac{\delta n}{N_e}\cos(kx)\right] f_M(v). \qquad (7)$$

This corresponds to a Maxwellian distribution $f_M(v)$ with a sinusoidal density perturbation along the x-direction, which evolves into a standing EPW. The relative density perturbation is set to $\delta n/N_e = 1 \times 10^{-4}$ to ensure the simulations remain in the linear regime.

In the linear regime, the decay of the EPW is, as expected, well fit with an exponential decay. Real frequencies ω_R and damping rates ν of the EPW for $k\lambda_{De} = 0.3$ and for a range values of $\nu_{ei,th}/\omega_{pe}, 0$ to $5\cdot10^{-1}$, are summarized in Fig. 1. Assuming $\ln(\Lambda_{ee}) \simeq \ln(\Lambda_{ei})$, the relation of $\nu_{ee,th}$ to $\nu_{ei,th}$ is taken to be $\nu_{ee,th} \simeq 4\,\nu_{ei,th}/Z$. Results have been obtained successively for $Z = 1$, 6, and 16. Also shown is the linear Landau damping rate, $\nu_{L,kin}/\omega_{pe} = 1.26 \times 10^{-2}$, for $k\lambda_{De} = 0.3$ in a collisionless plasma. Figure 1(a) shows that $\Delta\omega = \omega_R - \omega_{R,kin}$ decreases as $\nu_{ei,th}$ increases where $\omega_{R,kin} = 1.16\omega_{pe}$ is the linear frequency in a collisionless plasma ($\nu_{ei,th} = 0$). Thus the phase velocity decreases with increasing $\nu_{ei,th}$ and the linear Landau damping estimated with the frequency ω_R modified by finite collisionality thus increases with $\nu_{ei,th}$. However, we find this effect is not significant.

In the case of ion acoustic waves, Epperlein *et al.*[21] found a reduction in electron Landau damping from pitch-angle scattering of electrons from ions for $k\lambda_{ei} = kv_{\rm th}/\nu_{ei,th} < 1$ and a reduction in the collisional damping for $k\lambda_{ei} > 1$. The total electron damping remained greater than the Landau rate until $k\lambda_{ei} \ll 1$. This limit requires $\nu_{ei,th}/\omega_{pe} > k\lambda_{De}$, and thus is not accessible to EPWs with significant Landau damping rates.

Fig. 1(b) shows the EPW damping rate ν increases significantly once $\nu_{ei,th}/\omega_{pe} \gtrsim 0.01$. For constant $\nu_{ei,th}$, ν is larger for smaller Z, that is if $\nu_{ee,th} \gtrsim \nu_{ei,th}$. On the other hand, once $Z \gtrsim 6$ and $\nu_{ee,th} \lesssim \nu_{ei,th}$, this total damping rate is mainly dependent on $\nu_{ei,th}$ and $k\lambda_{De}$.

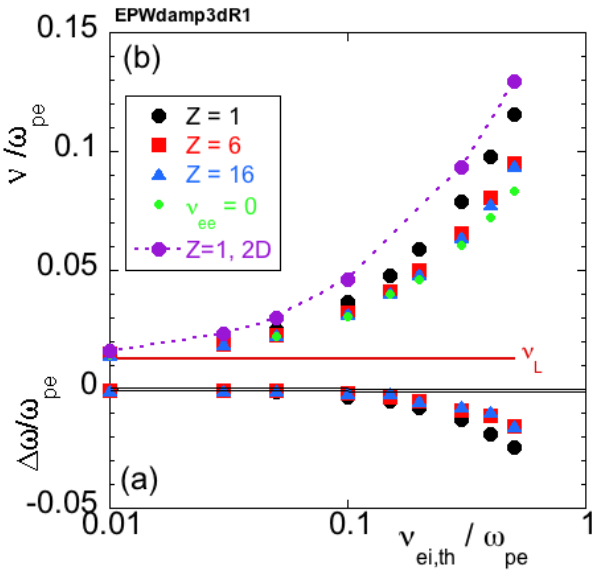

FIG. 1: (a) The frequency difference, $\Delta\omega = \omega_R - \omega_{R,kin}$, and (b) the total EPW damping rate, ν, is shown as a function of $\nu_{ei,th}/\omega_{pe}$ for $Z = 1, 6, 16$ and $k\lambda_{De} = 0.3$. The solid double horizontal line separates Figs (a) and (b). For higher Z values, the electron-ion scattering is the dominant source of collisional damping. The linear Landau damping rate ν_L for $k\lambda_{De} = 0.3$ in a collisionless plasma is shown in (b) by the horizontal solid red line. The result with pitch-angle collisions ($\nu_{ei} \neq 0$) but no self-collisions ($\nu_{ee} = 0$, *i.e.* $Z = \infty$) is also shown. For $Z = 1$ the damping from a LOKI simulation restricted to 2V Cartesian velocity coordinates is also shown.

Because collisions have a small effect on the linear Landau damping, the collisional component of the damping rate shown in Fig. 2 can be calculated as $\nu - \nu_{L,kin}$. The collisional damping rate, $\nu_{coll}^{fl} = \nu_{ei}^{brag}/2$, obtained from the hydrodynamic description is also shown for comparison. For $Z = 16$, as shown in Fig. 2(b), ν_{coll}^{fl} is up to 50% larger than the simulation result, particularly for larger values of $\nu_{ei,th}$. For lower ionization degrees, in particular $Z = 1$ shown in Fig. 2(a), ν_{coll}^{fl} agrees well with the kinetic simulations. This observation is explained by the fact that self-collisions being relatively important in this latter case, the distribution is maintained close to a shifted Maxwellian, which is the underlying assumption for the friction force relation in the Branginskii fluid equations [15].

In the limit that self-collisions are unimportant ($Z \to \infty$), an alternative approach to obtaining the kinetic frequency and damping of EPWs is afforded by the partial fraction technique[9, 12, 13, 21]. The plasma dispersion equation for EPWs including only electron-ion pitch angle collisions in 2V and 3V velocity space is found by a Legendre/Fourier series expansion of the linearized

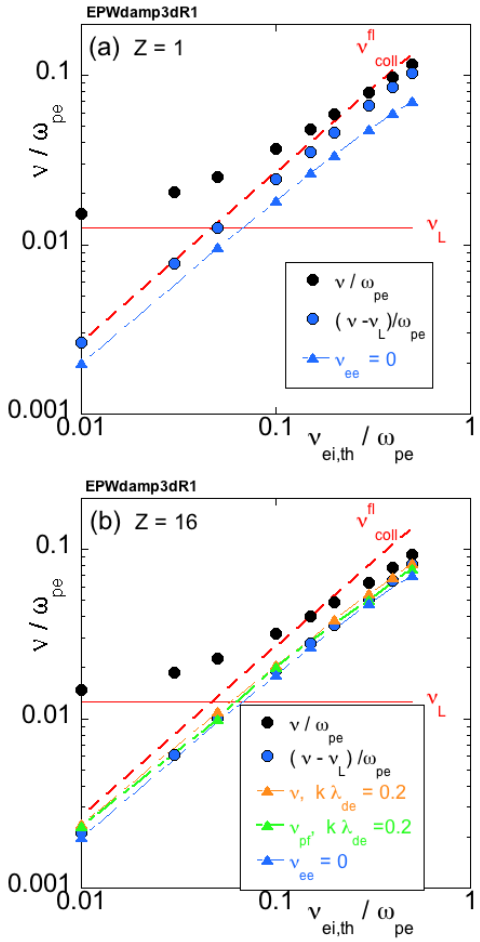

FIG. 2: The total (ν/ω_{pe}) and the collisional component of the damping rate of EPWs for (a) $Z = 1$ and (b) $Z = 16$ for $k\lambda_{De} = 0.3$. The linear Landau damping rate, $\nu_{L,kin}$ for $k\lambda_{De} = 0.3$ is displayed as a horizontal line. The collisional component of the Vlasov simulation damping rate $\nu_{coll} = \nu - \nu_{L,kin}$ for $k\lambda_{De} = 0.3$ is shown along with the hydrodynamic damping rate, ν^{fl}_{coll} (red dashed). Also displayed in (b) is the total damping rate for $k\lambda_{De} = 0.2$ which is essentially the same as the collisional component for $k\lambda_{De} = 0.3$ as the Landau damping for $k\lambda_{De} = 0.2$ is exceedingly small. The numerical solution to Eqs. (8)-(11) for $k\lambda_{De} = 0.2$ (ν_{pf}) is shown in (b). It agrees very well with the corresponding Vlasov simulation result in (b) and with the Vlasov simulation result for $Z = \infty$, that is, $\nu_{ee} = 0$.

Vlasov-Fokker-Planck equation with the result,[16]

$$\epsilon(k,\omega) = 1 + \chi_e(k,\omega) = 0, \quad (8)$$

$$\chi_e(k,\omega) = 2(V-1)\pi \int_0^\infty dv\, v^{V-1} \frac{v^2 f_M(v)}{k^2v^2 - Vi\omega\tilde{\nu}_1}, \quad (9)$$

where $V = 2$ and $V = 3$ for two or three dimensional velocity space respectively. The complex frequency $\tilde{\nu}_1$ is obtained in 2V and 3V by evaluating respectively the recurrence relations (10) and (11):

$$\tilde{\nu}_{l-1} = -i\omega + (l-1)^2\nu_{ei} + \frac{k^2v^2}{4\tilde{\nu}_l} \quad ; l \geqslant 2, \quad (10)$$

$$\tilde{\nu}_{l-1} = -i\omega + l(l-1)\nu_{ei} + \frac{l^2}{4l^2-1}\frac{k^2v^2}{\tilde{\nu}_l} \quad ; l \geqslant 2, \quad (11)$$

having defined $\nu_{ei}(v) = \nu_{ei,th}(v_{\rm th\,e}/v)^3$. Solving the dispersion relation (8)-(11) numerically for $V = 3$ results in excellent agreement with the Vlasov simulations with $\nu_{ee} = 0$ shown here. For $V = 2$, prior LOKI simulations that only included pitch-angle collisions also showed good agreement with the numerical solution of Eqs. (8),(9), and (10).[16]

The reduction of the damping with respect to the fluid result, ν^{fl}_{coll}, is most evident by examining the integrand in Eq. (9) which together with Eq. (8) is the plasma dispersion function when $\nu_{ee} = 0$, that is when $Z \to \infty$. In Appendix B1 of Reference ([16]) the solution of the dispersion relation, Eqns. (8-9) are discussed for the case that Landau damping is negligible. There it is shown that reduction is caused by the strong velocity dependence of the collision frequency, $\nu_{ei}(v) \propto \nu_{ei,th}v^{-3}$. As $\nu_{ei,th}$ increases, the imaginary part electron susceptibility is increasingly weighted by higher velocities and thus a lower effective collision frequency. In the limit that $Z \to 1$, that is, $\nu_{ee,th} \simeq \nu_{ei,th}$, the perturbation is constrained to be a shifted Maxwellian such that the hydrodynamic treatment is valid and the effective collision frequency is $\nu_{ei,th}$.

We have extended our simulations to other values of $k\lambda_{De}$, in particular to $k\lambda_{De} < 0.2$, smaller values more pertinent to TPD and forward SRS for which Landau damping is nearly insignificant. The EPW damping from the 1D+3V Vlasov simulations for $k\lambda_{De} = 0.2$, shown in Fig. 2(b), is a little larger than the collisional component of the damping for $k\lambda_{De} = 0.3$, reflecting a weak dependence of ν_{coll} on $k\lambda_{De}$ as well. Also in Fig. 2(b), the partial fraction solution for ν ("pf" in figure) is in excellent accord with the simulation results for $k\lambda_{De} = 0.2$.

For $Z \gg 1$, ν_{coll} decreases with k^2. With the onset of Landau damping (*i.e.* $k\lambda_{De} \sim 0.25$ for $\nu_{ei,th}/\omega_{pe} = 0.01$ and $k\lambda_{De} \sim 0.2$ for $\nu_{ei,th}/\omega_{pe} = 0.001$), the calculation of ν_{coll} is inaccurate (involving the subtraction of two nearly equal numbers). However, the decrease with k^2 likely continues such that for $k\lambda_{De} = 0.5$, the collisional component of the damping would be $\sim 0.5\nu^{fl}_{coll}$ in the case that $\nu_{ei,th}/\omega_{pe} = 0.001$. For $Z = 1$, no variation of ν_{coll} with k^2 was found for $k\lambda_{De} < 0.25$. These results are summarized in Fig. 3. Note, the $Z = 16$ collisional damping rate is well approximated by the $Z = \infty$ rate for which electron-electron self-collisions play no role. Shown in the blue and red lines for $\nu_{ei,th}/\omega_{pe} = 0.001$ and $\nu_{ei,th}/\omega_{pe} = 0.01$ are the fits to the $Z = \infty$ collisional damping rates given by $\nu_{coll}/\nu^{fl}_{coll} = 0.98 - 1.8(k\lambda_{De})^2$ and $\nu_{coll}/\nu^{fl}_{coll} = 0.96 - 2.1(k\lambda_{De})^2$ respectively.

The approach to the high-Z limit of collisional damping is quite rapid as shown in Fig. 4 for 3 values of col-

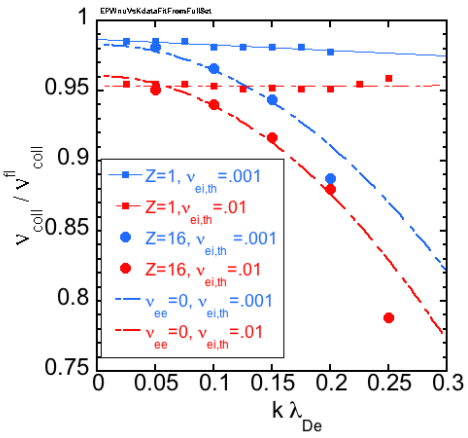

FIG. 3: The collisional component of the damping normalized to the fluid rate ν_{coll}^{fl} as a function of $k\lambda_{De}$. For $Z = 16$, the collisional damping rate decreases with $k^2\lambda_{De}^2$ for both $\nu_{ei,th}/\omega_{pe} = 0.01$ and $\nu_{ei,th}/\omega_{pe} = 0.001$. For $Z = 1$, the collisional damping rate is apparently independent of $k\lambda_{De}$ for both $\nu_{ei,th}/\omega_{pe} = 0.01$ and $\nu_{ei,th}/\omega_{pe} = 0.001$. The $Z = 16$ damping rate is well approximated by the $Z = \infty$ ($\nu_{ee} = 0$) results shown by the blue and red lines for $\nu_{ei,th}/\omega_{pe} = 0.001$ and $\nu_{ei,th}/\omega_{pe} = 0.01$ respectively.

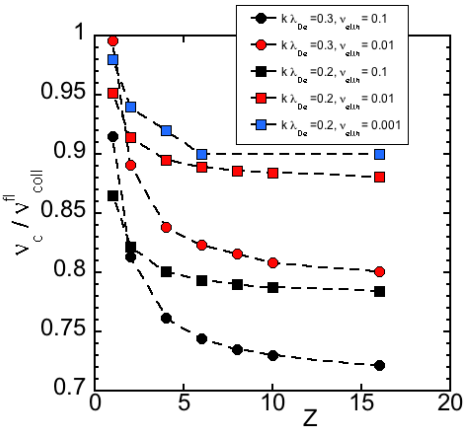

FIG. 4: The collisional component of the damping normalized to the fluid rate ν_{coll}^{fl} as a function of Z. For $Z > 10$ and $k\lambda_{De} = 0.3$, the collisional damping rate is $\nu_{coll} \sim 0.7\ \nu_{coll}^{fl}$ and $\nu_{coll} \sim 0.8\ \nu_{coll}^{fl}$ for $\nu_{ei,th} = 0.1$ and $\nu_{ei,th} = 0.01$ respectively. For $Z > 10$ and $k\lambda_{De} = 0.2$, the collisional damping rate is $\nu_{coll} \sim 0.8\ \nu_{coll}^{fl}$ for $\nu_{ei,th} = 0.1$ and $\nu_{coll} \sim 0.9\ \nu_{coll}^{fl}$ for $\nu_{ei,th} \lesssim 0.01$.

lision rate, $\nu_{ei,th}/\omega_{pe} = 0.1, 0.01, .001$ and 2 values of $k\lambda_{De} = 0.2$ and 0.3. As $Z \to 1$, the collisional damping rate, $\nu_{coll} \to \nu_{ei}^{brag}/2$. However, if $Z > 6$, ν_{coll} is only 70% of ν_{coll}^{fl} for strong collision rates but increases to 90% for weak collision rates. For weaker collision rates ($\nu_{ei,th}/\omega_{pe} < 0.01$), the collisional damping rate relative to ν_{coll}^{fl} ceases to change significantly for a given Z and $k\lambda_{De}$.

IV. DISCUSSION

We used a nonlinear 1D+3V Vlasov-Fokker-Planck code to obtain the Landau and collisional damping of EPWs, and showed that the collisional component of the damping relative to the collision rate $\nu_{ei,th}$ is dependent on the relative strength of electron-ion pitch-angle scattering to thermalization from electron-electron collisions,that is the charge state Z, the wavenumber $k\lambda_{De}$, and the ratio of the collision rate to the plasma frequency, $\nu_{ei,th}/\omega_{pe}$.

For ICF, one practical impact of the reduced collisional damping of EPWs is on the threshold laser intensity, I_L, for onset of TPD in direct-drive designs for MegaJoule scale laser facilities, such as NIF[22]. The estimated plasma scale lengths are so large that the TPD threshold is set by the collisional damping, $\gamma_0^{TPD} \propto \sqrt{I_L} > \nu_{coll}/2$ if Z is large enough, *e.g.* $Z \gtrsim 14$.[4] For the parameters given in Ref. [4], $k\lambda_{De} < 0.3$, the collisional rates are very small ($\nu_{ei,th}/\omega_{pe} \lesssim 10^{-3}$), and we estimate $\nu_{coll} \sim 0.9\,\nu_{coll}^{fl}$ or a 20 % reduction in the threshold laser intensity for TPD. The Langmuir decay instability is considered a saturation process for TPD as it has a low threshold if the daughter Langmuir wave is weakly Landau damped.[23, 24]. The threshold EPW wave amplitude, $(\delta n/n)_{LDI} \propto \sqrt{\nu_{iaw}\nu_{epw}}$, is determined by Landau damping of the ion acoustic wave, ν_{iaw}, and collisional damping of the EPW, ν_{epw}. The wavenumber dependence of the collisional damping of EPWs presented here may have an influence on the spectrum of waves nonlinearly driven. Much stronger collisional effects with $\nu_{ei,th}/\omega_{pe} \sim 0.1$ occur in low temperature plasmas where $T_e \sim 2$eV and $N_e \sim 10^{17}\mathrm{cm}^{-3}$[25].

Our results here address linear (small-amplitude) waves; the nonlinear evolution of an EPW including collisional de-trapping will be addressed in future work. In such nonlinear simulations, the rate of de-trapping depends on the scattering process, *i.e.* pitch-angle, drag, or parallel diffusion. Note that in the case of IAWs, the collisional de-trapping rates of ions and electrons scale differently from the de-trapping rate of electrons in an EPW.[26] For both EPWs and IAWs, large amplitude waves nonlinearly heat the plasma by collisional and collisionless processes anisotropically. Thus, it is essential to implement a collision operator as we have that is not limited a to Lorentzian pitch-angle[16] nor to a one-dimensional approximation[27] to Landau collision operator.

Plasma waves driven in laser speckles or by intrinsically 2D parametric instabilities such as TPD or SRS sidescatter require at least two Cartesian spatial dimensions and, to include collisions, a choice of reduced 2V Cartesian (v_x, v_y) or full 3V (v_x, v_y, v_z). An Eulerian representation in six-dimensional [or even five-dimensional (2D+3V)] phase space remains computationally prohibitive. Using

LOKI, [28, 29] a 2D+2V Vlasov-Fokker-Planck code in Cartesian geometry, similar results have been obtained to those obtained here in 3V; only the numerical coefficients are different (see Fig. 1).

V. ACKNOWLEDGMENTS

We are pleased to acknowledge valuable discussions with T. Chapman. This work was performed under the auspices of the U.S. Department of Energy by Lawrence Livermore National Laboratory under Contract DE-AC52-07NA27344 and funded by the Laboratory Research and Development Program at LLNL under project tracking codes 12-ERD-061 and 15-ERD-038. Computing support for this work came from the Lawrence Livermore National Laboratory (LLNL) Institutional Computing Grand Challenge program.

[1] V. M. Malkin, G. Shvets, and N. J. Fisch, Phy. Rev. Lett. **82**, 4448 (1999).
[2] D. S. Clark and N. J. Fisch, Phys. Plasmas **10**, 3363 (2003).
[3] W. Seka, D. H. Edgell, J. F. Myatt, A. V. Maximov, R. W. Short, V. N. Goncharov, and H. A. Baldis, Phys. Plasmas **16**, 052701 (2009).
[4] J. F. Myatt, J. Zhang, J. A. Delettrez, R. W. Short, W. Seka, D. H. Edgell, D. F. DuBois, D. A. Russell, and H. X. Vu, Phys. Plasmas **19**, 022707 (2012).
[5] R. S. Craxton, K. S. Anderson, T. R. Boehly, V. N. Goncharov, D. R. Harding, J. P. Knauer, R. L. McCrory, P. W. McKenty, D. D. Meyerhofer, J. F. Myatt, et al., Phys. Plasmas **22**, 110501 (2015).
[6] R. K. Follett, J. A. Delettrez, D. H. Edgell, V. N. Goncharov, R. J. Henchen, J. Katz, D. T. Michel, J. F. Myatt, J. Shaw, A. A. Solodov, et al., Phys. Rev. Lett. **116**, 155002 (2016).
[7] C. H. Su and C. Oberman, Phys. Rev. Lett. **20**, 427 (1968).
[8] S. P. Auerbach, Phys. Fluids **20**, 1836 (1977).
[9] A. Bendib, Phys. Rev. E **47**, 3598 (1993).
[10] J. Zheng and H. Qin, Phys. Plasmas **20**, 092114 (2013).
[11] J. D. Callen, Phys. Plasmas **21**, 052106 (2014).
[12] A. V. Brantov, V. Y. Bychenkov, W. Rozmus, and C. E. Capjack, Phys. Rev. Lett. **93**, 125002 (2004).
[13] A. V. Brantov, V. Y. Bychenkov, and W. Rozmus, Phys. Rev. Lett. **108**, 205001 (2012).
[14] N. A. Krall and A. W. Trivelpiece, *Principles of Plasma Physics* (McGraw-Hill Book Company, New York, 1973), p. 135, International series in pure and applied physics.
[15] S. I. Braginskii, *Particle Interactions in a Fully Ionized Plasma* (M. A. Leontovich, Consultants Bureau, New York, 1965), vol. 1 of *Reviews of Plasma Physics*, p. 205.
[16] J. W. Banks, S. Brunner, R. L. Berger, and T. M. Tran, Phys. Plasmas **23**, 032108 (2016).
[17] M. N. Rosenbluth, W. M. MacDonald, and D. L. Judd, Phys. Rev. **107**, 1 (1957).
[18] S. Brunner, E. J. Valeo, and J. Krommes, Phys. Plasmas **6**, 4504 (1999).
[19] Z. Lin, W. M. Tang, and W. W. Lee, Phys. Plasmas **2**, 2975 (1995).
[20] R. A. Kolesnikov, W. X. Wang, and F. L. Hinton, Journal of Computational Physics **229**, 5564 (2010).
[21] E. M. Epperlein, R. W. Short, and A. Simon, Phys. Rev. Lett. **69**, 1765 (1992).
[22] W. J. Hogan, E. I. Moses, B. E. Warner, M. S. Sorem, and J. M. Soures, Nucl. Fusion **41**, 567 (2001).
[23] R. K. Kirkwood, B. J. MacGowan, D. S. Montgomery, B. B. Afeyan, W. L. Kruer, J. D. Moody, K. G. Estabrook, C. A. Back, S. H. Glenzer, M. A. Blain, et al., Phys. Rev. Lett. **77**, 2706 (1996).
[24] K. L. Baker, R. P. Drake, B. S. Bauer, K. G. Estabrook, A. M. Rubenchik, C. Labaune, H. A. Baldis, N. Renard, S. D. Baton, E. Schifano, et al., Phys. Plasmas **4**, 3012 (1997).
[25] A. N. Mostovych and A. W. DeSilva, Phys. Rev. Lett. **53**, 1563 (1984).
[26] R. L. Berger, S. Brunner, T. Chapman, L. Divol, C. H. Still, and E. J. Valeo, Phys. Plasmas **20**, 032107 (2013).
[27] A. Lenard and I. B. Bernstein, Phys. Rev. **112**, 1456 (1958).
[28] J. W. Banks and J. A. F. Hittinger, IEEE T. Plasma. Sci. **38**, 2198 (2010).
[29] J. W. Banks, R. L. Berger, S. Brunner, B. I. Cohen, and J. A. F. Hittinger, Phys. Plasmas **18**, 052102 (2011).